

# Temperature dependence of ferroelectric properties and the activation energy of polarization reversal in (Pr,Mn)-codoped BiFeO<sub>3</sub> thin films

メタデータ	言語: eng 出版者: 公開日: 2017-10-03 キーワード (Ja): キーワード (En): 作成者: メールアドレス: 所属:
URL	<a href="https://doi.org/10.24517/00009236">https://doi.org/10.24517/00009236</a>

This work is licensed under a Creative Commons Attribution-NonCommercial-ShareAlike 3.0 International License.



# Temperature dependence of ferroelectric properties and the activation energy of polarization reversal in (Pr,Mn)-codoped BiFeO<sub>3</sub> thin films

Yukihiro Nomura<sup>1</sup>, Takashi Tachi<sup>1</sup>, Takeshi Kawae<sup>2</sup> and Akiharu Morimoto<sup>\*,2</sup>

<sup>1</sup> Graduate school of Natural Science and Technology, Kanazawa University, Kakuma-machi, Kanazawa, Ishikawa, 920-1192, Japan

<sup>2</sup> College of Science and Engineering, Kanazawa University, Kakuma-machi, Kanazawa, Ishikawa, 920-1192, Japan

Received ZZZ, revised ZZZ, accepted ZZZ

Published online ZZZ (Dates will be provided by the publisher.)

**Keywords** BiFeO<sub>3</sub>, PZT, polarization reversal, activation energy, low temperature

\* Corresponding author: e-mail amorimot@ec.t.kanazawa-u.ac.jp, Phone: +81 076 234 4876, Fax: +81 076 234 4870

We applied Vopsaroiu's model to (Bi,Pr)(Fe,Mn)O<sub>3</sub> (BPFM) and Pb(Zr,Ti)O<sub>3</sub> (PZT) ferroelectric thin films fabricated by chemical solution deposition. Temperature dependences of the saturation polarization and the coercive field were measured in low temperature region from 100 to 200 K. The saturation polarizations of BPFM thin films were decreased with decreasing the measurement temperature due to polarization pinning effect while that of PZT thin film was almost unchanged over the temperature region. The coercive fields of all the thin films

were increased linearly with decreasing the measurement temperature. The activation energies for polarization reversal in as-grown BPFM, post-annealed BPFM and PZT thin films were 1.18, 1.25, 0.95 eV, respectively. These results indicate that BPFM thin films have large activation energies for polarization reversal compared with PZT thin film. In addition, the post-annealed BPFM thin film has a larger activation energy than the as-grown BPFM thin film.

Copyright line will be provided by the publisher

**1 Introduction** Ferroelectric random access memory (FeRAM) has attracted much attention due to their non volatility, high speed operation, and low power consumption. However, Pb(Zr,Ti)O<sub>3</sub> (PZT) and SrBiTaO<sub>3</sub> (SBT) have no large polarization sufficient for reduced cell-size in LSI[1-7].

It has been revealed that BiFeO<sub>3</sub> (BFO) has a large polarization ( $P_r=100 \mu\text{C}/\text{cm}^2$ ) and a high Curie temperature ( $T_c=830 \text{ }^\circ\text{C}$ )[8-12]. Thus, the BFO is expected to be suitable for ferroelectric material in the highly-integrated and reliable FeRAM. However, it is known that BFO thin films have seriously large leakage current at room temperature, leading to a difficulty in the application[11,12]. Site-engineering technique and optimization of process condition were performed to improve their ferroelectric properties[12]. So far, the reasons of the improvements are, however, still open question. Thus, in order to reveal the origin of improvement in ferroelectric properties, systematic characterization is required by changing the measurement

parameters such as temperature and applied field. Here, since the leakage current disturbs the measurement of essential ferroelectric properties, low temperature measurements were performed in order to characterize the ferroelectric properties without influences of the leakage current[11].

On the other hand, it is known that BFO thin film has a large coercive field compared with PZT and SBT thin films[2,7,8]. Thus, it is expected that BFO thin films achieve the superior retention properties compared with other ferroelectric materials such as PZT and SBT thin films. In fact, we have demonstrated the superior retention properties with high-temperature resistance in (Pr,Mn)-codoped BiFeO<sub>3</sub> thin film capacitor[13]. The origin of their superior high-temperature resistance has, however, not been revealed. Thus, for understanding the basic properties of BFO thin films and the related materials, and for applying the those thin films to various devices, it is necessary to evaluate temperature dependence and electric field dependence of the ferroelectric properties.

Copyright line will be provided by the publisher

For analyzing and clarifying the ferroelectric properties, one of the pioneering theoretical models of the polarization switching is the Kolmogorov-Avrami-Ishibashi (KAI) domain nucleation-switching model. The KAI model was derived from the original Avrami nucleation model of crystal growth, and it describes the polarization reversal process as the first nucleation process and successive domain growth process[14-19]. The KAI model on polarization switching has successfully given a good description of polarization kinetics of ferroelectric single crystals and some epitaxial thin films[14,20]. However, the KAI model is not fully applicable to the polarization reversal behavior over larger time periods or in polycrystalline thin films[21,22]. Attempts to refine the KAI model in order to increase its applicability have been made by assuming a distribution of relaxation times, a nucleation-limited switching model and a statistical time-dependent depolarization field[21-24].

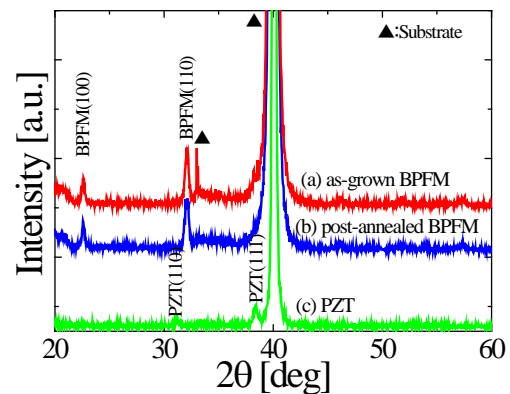
However, one of the major limitations of the KAI model or the modified versions is given by the failure to predict the relationship among the switching time, the applied electric field and the temperature. To overcome this issue, Vopsaroiu *et al.* proposed a polarization reversal model, considering thermal energy and applied electric field using a non-equilibrium statistical model [25]. In their model an analytic expression for the time and temperature dependences of the coercive field was given, and they successfully derived the coercive field as a function of the time and temperature.

In this article, we performed a systematic characterization of ferroelectric properties varying the temperature and applied field for (Pr,Mn) co-doped BFO (BPFM) thin films. In addition, we analyzed these result using Vopsaroiu's model. In order to improve the BPFM ferroelectric properties, we examined an influence of O<sub>2</sub> annealing for an as-grown BPFM thin film. From these results, we revealed detailed ferroelectric properties of BPFM thin films compared with a PZT thin film and the influence of O<sub>2</sub> annealing process of BPFM thin films.

**2 Experimental** In the present study, as a member of the BFO family, (B<sub>0.9</sub>Pr<sub>0.1</sub>)(Fe<sub>0.97</sub>Mn<sub>0.03</sub>)O<sub>3</sub> (BPFM) thin films were fabricated by chemical solution deposition (CSD) method[26]. BPFM solutions (Toshiba) were spin-coated at 3000 rpm for 30 s on Pt/TiO<sub>2</sub>/SiO<sub>2</sub>/Si(100) substrates, followed by a drying process at 120 °C for 15 min and a pyrolysis process at 430 °C for 10 min in atmosphere. These processes were repeated 10 times until the thin film thickness reached approximately 200 nm. The resultant thin films were then heat-treated for crystallization at 600 °C for 20 min in flowing N<sub>2</sub> gas. After the depositions, one thin film was annealed at 300 °C in O<sub>2</sub> flow for 60 min, and the thin film is denoted by post-annealed BPFM thin film hereafter. Another thin film is as-grown one, and it is denoted by as-grown BPFM thin film hereafter. For comparison, PZT thin films without a

post-annealing process were also fabricated by CSD method on Pt/TiO<sub>2</sub>/SiO<sub>2</sub>/Si(100) substrates, similarly to the BPFM thin films. Finally Au top electrodes with 100 μm in diameter were deposited by thermal evaporation, resulting in capacitor structures.

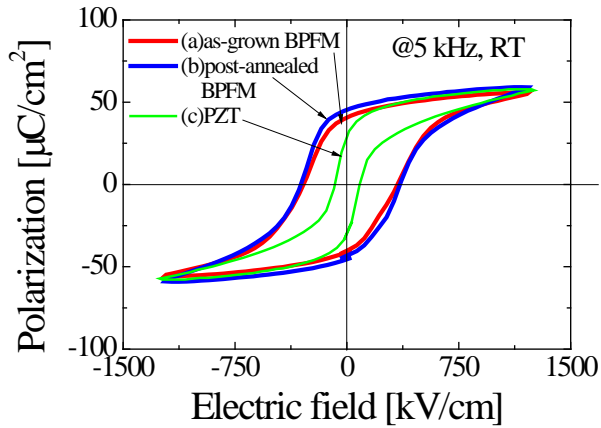
The crystal structure of the thin films was determined by an X-ray diffractometer (XRD) (Shimadzu XD-D1) with Cu K<sub>α</sub> radiation before deposition of Au top electrodes. The thin film thickness was measured by a spectroscopic ellipsometer (J. A. Woollam M-2000U). The polarization vs electric field (*P-E*) curves were measured by a ferroelectric test system (TOYO FCE-3) in liquid N<sub>2</sub> dewar vessel. The *P-E* curve measurements were performed in low temperature region from 100 to 200 K with a measurement frequency of 100 Hz and the maximum applied electric field of 1500 kV/cm after measurements at room temperature with a frequency of 5 kHz.



**Figure 1** XRD patterns for (a) as-grown BPFM, (b) post-annealed BPFM, and (c) PZT thin films.

**3 Results and discussion** Figure 1 shows XRD patterns of the as-grown BPFM, the post-annealed BPFM and the PZT thin films. As shown in Fig.1, BPFM thin films shows polycrystalline phases of perovskite without any impurity phases such as Bi<sub>2</sub>O<sub>3</sub> and Bi<sub>2</sub>Fe<sub>4</sub>O<sub>9</sub>. In addition, the PZT thin film also shows polycrystalline phases of perovskite without any pyrochlore phases.

Figure 2 shows *P-E* hysteresis loops of specimens measured at room temperature with a measurement frequency of 5 kHz. As shown in Fig.2, the thin films show clear hysteresis loops without influences of leakage current, indicating fairly good ferroelectric properties. In addition, there are no large differences in the hysteresis loop between the as-grown BPFM and post-annealed BPFM thin films while there is a large difference between the BPFM and PZT thin films. The coercive fields of the as-grown BPFM, the post-annealed BPFM and the PZT thin films are 320, 340, and 90 kV/cm, respectively.



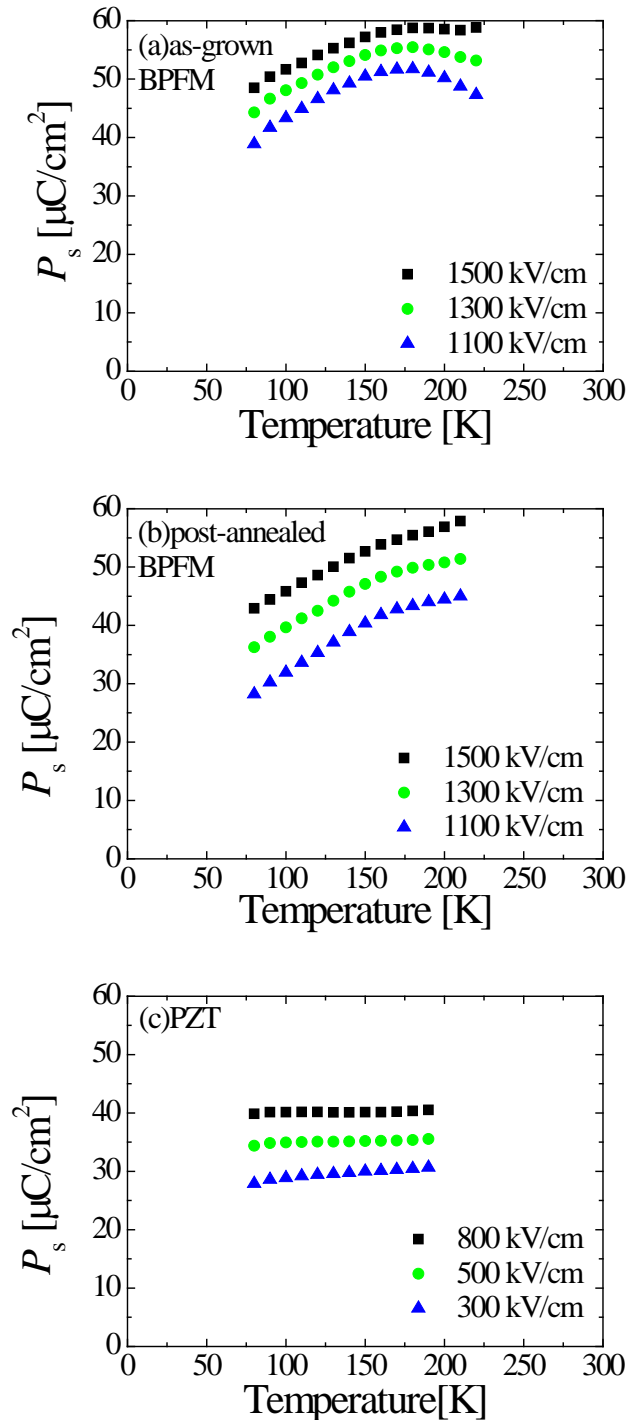
**Figure 2**  $P$ - $E$  curves with a measurement frequency of 5 kHz at RT for (a) as-grown BPFM, (b) post-annealed BPFM and (c) PZT thin films.

Figure 3 shows temperature dependences of the saturation polarization  $P_s$  of specimens. As shown in Figs.3(a) and 3(b), under the largest applied field,  $P_s$ 's of both the BPFM thin films were decreased with decreasing temperature. Similar behavior was observed in  $\text{Bi}_{0.9}\text{La}_{0.1}\text{FeO}_3$  thin films as well, suggesting this behavior is a versatile phenomenon in the BFO-related ferroelectrics[27]. These phenomena as shown in Figs.3(a) and 3(b) are ascribed to be a pinning effect for polarization at low temperature. In contrast, as shown in Fig. 3(c) there is no temperature dependence of  $P_s$  in the PZT thin film. This remarkable difference in the temperature dependence of  $P_s$  between BPFM and PZT thin films in low temperature region seems to be originating from the difference in the pinning effect deduced from temperature dependences of the coercive field  $E_c$  between these thin films described below.

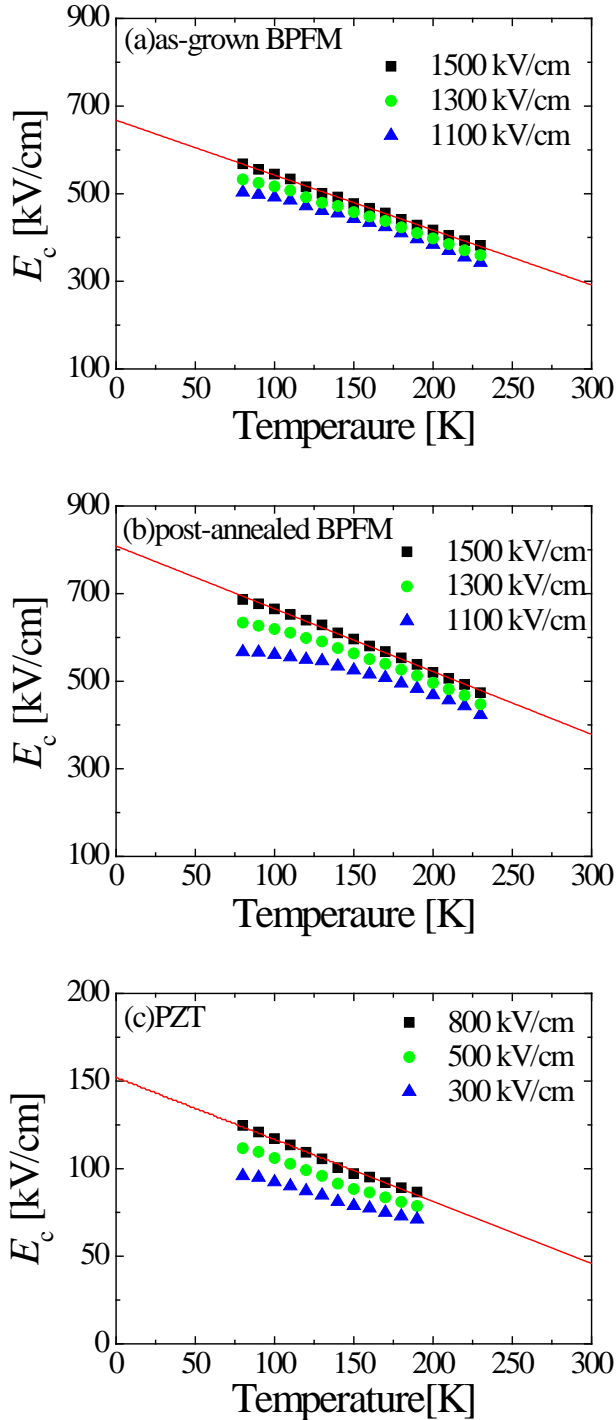
There is a peak in  $P_s$  vs  $T$  for a small applied field in Fig 3 (a). The reason is not clear at present. However, it is deduced that a back-switching phenomenon takes place especially at relatively high temperature regime when the applied field is not far larger than the  $E_c$  value.

Figure 4 shows temperature dependences of the coercive field  $E_c$  in the BPFM and PZT thin films measured with three maximum applied electric fields for each. As shown in Fig.4, the temperature dependences of  $E_c$  were different from those of  $P_s$ . The coercive field  $E_c$  in all thin films was monotonously increased with decreasing the measurement temperature, except for data obtained at the smallest applied field. These behaviors were almost similar to previous reports such as  $\text{PbZr}_{0.5}\text{Ti}_{0.5}\text{O}_3$  and  $\text{SrBi}_2\text{Ta}_2\text{O}_9$ [28-30]. However, the temperature dependences of  $E_c$  in Fig.4 have superior linearity compared with those of the previous reports. It is suggested that the large maximum applied fields affect the superior linearity. In fact, note that the temperature dependences of  $E_c$  at the small maximum applied field have inferior linearity. The reason for these deviations from the linear behavior is the fact that Eq. (1) representing the linear behaviors, described below, is valid for maxi-

imum applied fields that can produce polarization reversal and are much larger than the  $E_c$  values. The closer the maximum applied field is to  $E_c$ , the stronger is the deviation from linearity.



**Figure 3** Measurement-temperature dependences of the saturation polarization  $P_s$  with a measurement frequency of 100 Hz for (a) as-grown BPFM, (b) post-annealed BPFM and (c) PZT thin films.



**Figure 4** Measurement-temperature dependences of the coercive field  $E_c$  with a measurement frequency of 100 Hz for (a) as-grown BPFM, (b) post-annealed BPFM and (c) PZT thin films. Solid symbols and straight lines show measured data and calculated results using Eq.(1), respectively. The straight lines are only for data obtained at the maximum applied electric field in each specimen.

In addition, as shown in Figs.4(a) and (b), the temperature dependence of  $E_c$  of the post-annealed BPFM thin film was rather large compared with that of the as-grown BPFM thin film. This result agrees the result shown in Figs. 3(a) and 3(b) that the temperature dependence of  $P_s$  in the post-annealed thin film was slightly large compared with those in the as-grown thin film. Besides,  $E_c$  in PZT thin film in whole temperature region has rather small  $E_c$  compared with those in BPFM thin films.

Because of the strong pinning effect in the BPFM thin films compared with the PZT thin film, the polarization reversal was suppressed at low temperature. Thus, this result agrees well the result shown in Fig.3 that the temperature dependences of  $P_s$  in the BPFM thin films are larger than those in the PZT thin film. In addition, the temperature dependence of  $E_c$  in the BPFM thin film is enhanced by post-annealing process, suggesting that the pinning effect is enhanced strongly by the post-annealing process.

As shown in Fig.3 and Fig.4, there were large differences in temperature dependences of  $P_s$  and  $E_c$ , which were influenced by pinning effect[27, 31]. It is unclear how the domain pinning quantitatively influences the ferroelectric properties. Therefore, we analyzed the experimental results using Vopsariou's model,

$$E_c(T) = \frac{W_B}{P_s} - \frac{k_B T}{P_s V^*} \ln\left(\frac{\nu_0 t}{\ln 2}\right), \quad (1)$$

where  $W_B$  is the energy barrier per unit volume for the polarization reversal,  $V^*$  is the critical domain volume of the elementary nucleation site,  $k_B$  is Boltzmann's constant,  $\nu_0$  is the phonon frequency, and  $t$  is the measurement time. For the derivation of the formula, Vopsariou *et al.* used the model as shown in Figure 5

State 1 and state 2 represent the polarization states of upward and downward, and  $W_B$  is the energy barrier height for polarization reversal per unit volume at the time of transition between the two states when the external electric field is zero ( $E_{app}=0$ ) as shown in Fig.5 (a). In addition, when  $E_{app}=0$  state,  $W_B$  is rather large compared with the thermal energy  $k_B T$ , Thus, it takes long period for polarization reversal. When an electric field was applied, one polarization becomes stable depending on the direction of the applied field, as shown in Eq. (2),

$$W_{1,2} = (-W_B \mp P_s E_{app}) V^*. \quad (2)$$

Here,  $W_1$  and  $W_2$  are the free energies of state 1 and state 2, respectively, when positive or negative external electric field  $E_{app}$  is applied. Assuming the initial state is in state 1, a transition from state 1 to state 2 is expected after applying negative bias ( $E_{app}<0$ ) because the free energy of state 2 is lower than that of state 1 ( $W_2<W_1$ ) as shown in Fig.5(b). In contrast, the polarization state remains in state 1 after applying positive bias ( $E_{app}>0$ ) because  $W_1<W_2$  as shown in Fig.5(c).

The experimental data on the temperature dependences of the coercive field  $E_c$  give us the straight line fits with intercepts and slopes as shown in Fig.4. For obtaining the  $W_B$  value from the simulated results based on Eq.(1), the  $P_s$

value is required. The  $P_s$  values for the as-deposited BPFM thin film, the post-annealed BPFM and PZT thin films were assumed to be 58.5, 56.8 and 40.1  $\mu\text{C}/\text{cm}^2$  obtained at about 200 K in Fig.3, respectively. These values were adopted as the maximum values in the present measurement temperature region, because  $P_s$  was defined as reversible polarization, or spontaneous polarization in original Vopsaroiu's model. Here, for simplicity, we employed the maximum saturation polarization  $P_s$  experimentally obtained, instead of the spontaneous polarization of Vopsaroiu's model.

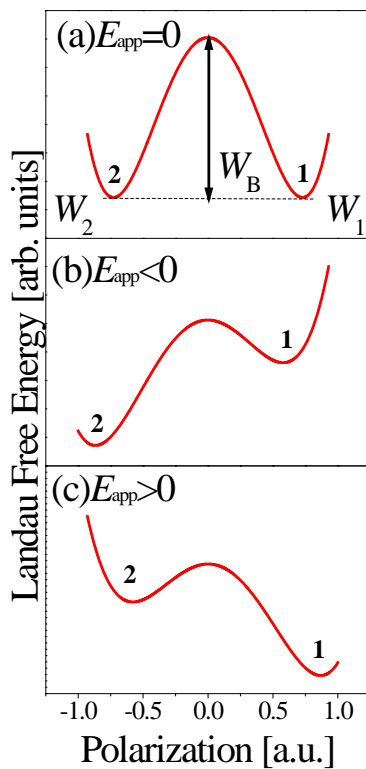


**Figure 5** Energy profiles of the polarization at different applied electric fields, (a)  $E_{app}=0$ , (b)  $E_{app}<0$ , and (c)  $E_{app}>0$ .

Actually, when determining  $P_s$ ,  $P$ - $E$  curves at the maximum applied electric field for each thin film was used. In order to derive the critical volume  $V^*$  from the slope in temperature dependences of  $E_c$ ,  $P_s$  was obtained as illustrated previously, the measurement time  $t$  was calculated from the inverse sweep frequency of the  $P$ - $E$  measurement, and the phonon frequency  $\nu_0$  is assumed to be  $10^{12}$  Hz. Calculated results using the experimental results shown in Figs. 3 & 4 and simulation employing Eq. (1) were shown in Table I. As shown in the table, the post-annealed BPFM thin film has a small  $V^*$  and a large  $W_B$  compared with the

as-grown BPFM thin film. The activation energy per critical volume  $V^*$  of the as-grown BPFM and post-annealed BPFM thin films,  $W_B V^*$ , were 1.18, 1.25 eV, respectively. On the other hand, the PZT thin film has a rather small  $W_B$ , a rather large  $V^*$  and a small activation energy  $W_B V^*$  of 0.95 eV. The activation energy of the PZT thin film is close to the value of PZT ceramics previously reported by A. Yu. Belov *et al.* using a thermally activation model of domain wall motions[32].

By transforming Eq. (1), we obtained Eq. (3).

$$\frac{E_c(T)}{E_c(0)} = 1 - \frac{k_B T}{W_B V^*} \ln \left( \frac{\nu_0 t}{\ln 2} \right), \quad (3)$$

where  $E_c(0) = W_B / P_s$ . If all the measurement conditions are the same, the inverse slope of temperature dependence of coercive field is proportional to  $W_B V^*$ . In addition,  $W_B V^*$  is the energy barrier, or the activation energy, that must be overcome thermally for the polarization reversal. Large  $W_B V^*$  indicates that the thermal polarization reversal of a certain material is difficult.

**Table 1** Calculated parameters using the experimental results shown in Figs. 3 & 4 and simulation employing Eq. (1).

	$P_s$ [ $\mu\text{C}/\text{cm}^2$ ]	$W_B$ [ $10^{26}$ eV/ $\text{m}^3$ ]	$V^*$ [ $10^{-27}$ $\text{m}^3$ ]	$W_B V^*$ [eV]
(a) as-grown BPFM	58.5	2.4	4.9	1.18
(b) post-annealed BPFM	56.8	2.9	4.4	1.25
(c) PZT	40.1	0.38	25	0.95

Therefore, we deduced that the difference in temperature dependence of  $P_s$  shown in Fig.3 is affected by the difference in the activation energy required for the polarization reversal. In other words,  $P_s$  of film with a large activation energy is largely dependent on the temperature while  $P_s$  of film a small activation energy is not largely dependent on the temperature.

The magnitude of the activation energy for the polarization reversal is known to be strongly affected by defects in the ferroelectric materials. From the view point, annealing process is expected to suppress the defect formation, resulting in a small activation energy. The present result seems to contradict this idea. However, Gong *et al.* reported a mechanism of precipitation in  $\text{YBa}_2\text{Cu}_3\text{O}_x$  thin film preparation[33]. They claimed that if a thin film is prepared under an equilibrated condition the crystal growth proceeds in local thermodynamic equilibration to form a well-equilibrated and relaxed crystal matrix accompanied by precipitation of defects at the thin film surface. If the thin film was prepared under the conditions deviated from the optimized one, precipitates should be incorporated into the thin film as defects. Thus the present result can be ascribed the possibility that the post-annealing process sweeps out a large number of defects from grains, resulting in precipitation of defects with the large activation energy.

In other words, small defects seem to be precipitated at grain boundaries by the post-annealing, resulting in strong pinning sites. Maximum-applied-electric-field dependences of  $P_s$  in the as-grown BPFM and post-annealed BPFM and the PZT thin films measured at 100 K are shown in Fig. 6. It is clearly shown that the polarization reversal is more difficult in the BPFM thin films than the PZT thin film. Comparing the polarization behaviors of BPFM thin films, remarkable differences are observed in the  $P_s$  value between the as-grown BPFM and post-annealed BPFM thin films in a medium applied electric field region while there are no differences at a sufficient applied electric field around 1500 kV/cm. Polarization reversal is more difficult in the post-annealed BPFM thin film than in the as-grown one. These results are consistent with the above-mentioned result that the activation energies of the BPFM thin films are larger than that of the PZT thin film, and the activation energy of BPFM thin film was increased by the post-annealing process. BPFM thin films are found to have larger activation energies for the polarization reversal compared with PZT thin films. This result indicates that BPFM thin films are more suitable for memory operation at high temperatures than PZT films. In addition, the post-annealed BPFM thin film is found to have larger activation energy than the as-grown BPFM thin film. This result also indicates that the post-annealed BPFM thin film is more suitable for memory operation at high temperatures than the as-grown BPFM thin film.

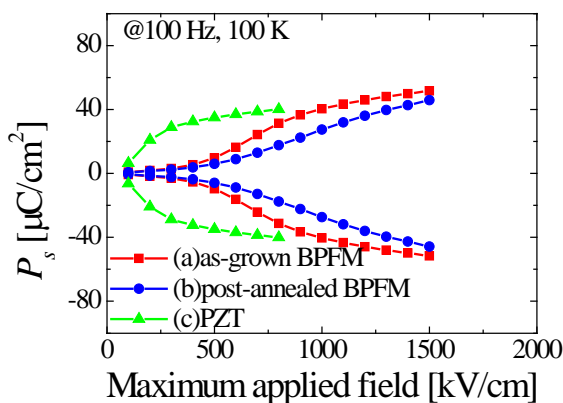


**Figure 6** Maximum-applied-field dependences of  $P_s$  at 100 K for (a) as-grown BPFM, (b) post-annealed BPFM and (c) PZT thin films.

**4 Conclusions** We applied Vopsaroiu's model on the polarization reversal to the ferroelectric properties of the BPFM and PZT thin films fabricated by CSD method. In addition, we investigated the effect of  $O_2$  post-annealing process on the ferroelectric properties of BPFM thin films.

The temperature dependence of the saturation polarization  $P_s$  in the BPFM thin films were evaluated at low temperature region and the behaviors were explained by the pinning effect of the polarization. The BPFM thin film showed that the  $P_s$  value is decreased by decreasing the

temperature while the PZT thin film showed the constant  $P_s$  value regardless of the measurement temperature. These results suggest the strong pinning effect in the BPFM thin films. On the other hand, the coercive fields of BPFM and PZT thin films were increased linearly with decreasing temperature. Based on the Vopsaroiu's model the critical domain volume  $V^*$  of the as-grown BPFM, the post-annealed BPFM, and the PZT thin films were  $4.9$ ,  $4.4$ ,  $25 \times 10^{-27} \text{ m}^3$ , respectively. The activation energy  $W_B V^*$  for polarization reversal in the as-grown BPFM, post-annealed BPFM and PZT thin films were  $1.18$ ,  $1.25$ ,  $0.95 \text{ eV}$ , respectively. These results indicated that BPFM thin films have large activation energies for polarization reversal and are suitable for high-temperature memory operation compared with PZT thin film. In addition, the post-annealed BPFM thin film is more preferable for high-temperature memory operation than the as-grown BPFM thin film.

**Acknowledgements** This work was partly supported by JSPS KAKENHI Grant Number 26630126.

## References

- [1] I. Stolichnov, A. K. Tagantsev, E. Colla, N. Setter, and J. S. Cross, *J. Appl. Phys.* **98**, 084106 (2005).
- [2] T. M. Kamel, F. X. N. M. Kools, and G. de With, *J. Eur. Ceram. Soc.* **27**, 2471 (2007).
- [3] B. S. Kang, D. J. Kim, J. Y. Jo, T. W. Noh, J. G. Yoon, T. K. Song, Y. K. Lee, J. K. Lee, S. Shin, and Y. S. Park, *Appl. Phys. Lett.* **84**, 3127 (2004).
- [4] W. Jo, D. C. Kim, and J. W. Hong, *Appl. Phys. Lett.* **76**, 390(2000).
- [5] S. Kim, J. Koo, S. Shin, and Y. Park, *Appl. Phys. Lett.* **87**, 212910(2005).
- [6] C. A-Paz de Araujo, J. D. Cuchiario, L. D. McMillan, M. C. Scott, and J. F. Scott, *Nature* **374**, 627(1995).
- [7] Y. Noguchi, H. Shimizu, M. Miyayama, K. Oikawa and T. Kamiyama, *Jpn. J. Appl. Phys.* **40**, 5812 (2001).
- [8] J. Wang, J. B. Neaton, H. Zheng, V. Nagarajan, S. B. Ogale, B. Liu, D. Viehland, V. Vaithyanathan, D. G. Schlom, U. V. Waghmare, N. A. Spaldin, K. M. Rabe, M. Wuttig, and R. Ramesh, *Science* **299**, 1719(2003).
- [9] D. Lebeugle, D. Colson, A. Forget, M. Viret, P. Bonville, J. F. Marucco, and S. Fusil, *Phys. Rev. B* **76**, 024116(2007).
- [10] V. V. Shvartsman, W. Kleemann, R. Haumont, and J. Kreisel, *Appl. Phys. Lett.* **90**, 172115(2007).
- [11] K. Y. Yun, D. Ricinchi, T. Kanashima, M. Noda, and M. Okuyama, *Jpn. J. Appl. Phys.* **43**, L647(2004).
- [12] T. Kawae, Y. Terauchi, T. Nakajima, S. Okamura and A. Morimoto, *J. Ceram. Soc. Jpn.* **118**, 652 (2010).
- [13] Y. Nomura, K. Nomura, K. Kinoshita, T. Kawae, and A. Morimoto, *Phys. Status Solidi RRL* **8**, 536(2014).
- [14] S. Hashimoto, H. Orihara, and Y. Ishibashi, *J. Phys. Soc. Jpn.* **63**, 1601 (1994).
- [15] H. Orihara, S. Hashimoto, and Y. Ishibashi, *J. Phys. Soc. Jpn.* **63**, 1031 (1994).
- [16] A. N. Kolmogorov, *Izv. Akad. Nauk SSSR Ser. Math.* **3**, 355(1937).
- [17] M. Avrami, *J. Chem. Phys.* **8**, 212(1940).

- 1 [18] V. Shur, E. Rumyantsev, and S. Makarov, *J. Appl. Phys.* **84**,  
2 445(1998).
- 3 [19] V. Shur, E. Rumyantsev, and S. Makarov, *Ferroelectrics*  
4 **172**, 361(1994).
- 5 [20] Y. W. So, D. J. Kim, T. W. Noh, J. G. Yoon, and T. K.  
6 Song, *Appl. Phys. Lett.* **86**, 092905(2005).
- 7 [21] J. Y. Jo, H. S. Han, J. G. Yoon, T. K. Song, S. H. Kim, and  
8 T. W. Noh, *Phys. Rev. Lett.* **99**, 267602(2007).
- 9 [22] A. K. Tagantsev, I. Stolichnov, N. Setter, J. S. Cross and M.  
10 Tsukada, *Phys. Rev. B* **66**, 214109(2002).
- 11 [23] O. Lohse, M. Grossmann, U. Boettger, D. Bolten, and R.  
12 Waser, *J. Appl. Phys.* **89**, 2332(2001).
- 13 [24] X. J. Lou, *J. Phys., Condens. Matter.* **21**, 012207 (2009).
- 14 [25] M. Vopsaroiu, J. Blackburn, M. G. Cain, and P. M. Weaver,  
15 *Phys. Rev. B* **82**, 024109(2010).
- 16 [26] T. Kawae, Y. Seto, and A. Morimoto, *Jpn. J. Appl. Phys.* **52**,  
17 04CH03(2013).
- 18 [27] Y. Wang and J. Wang, *J. Appl. Phys.* **106**, 094106(2009).
- 19 [28] X. J. Meng, J. L. Sun, X. G. Wang, T. Lin, J. H. Ma, S. L.  
20 Guo, and J. H. Chu, *Appl. Phys. Lett.* **81**, 4035(2002).
- 21 [29] G. L. Yuan, J.M. Liu, S. T. Zhang, D. Wu, Y. P. Wang, Z.  
22 G. Liu, H. L. W. Chan, and C. L. Choy, *Appl. Phys. Lett.*  
23 **84**, 954(2004).
- 24 [30] M. Vopsaroiu, P. M. Weaver, M. G. Cain, M. J. Reece, and  
25 K-B. Chong, *IEEE Transactions on Ultrasonics, Ferroelec-*  
26 *trics, and Frequency Control*, **58**, 1867 (2011).
- 27 [31] Y. Wang, K. F. Wang, C. Zhu, and J.M. Liu, *J. Appl. Phys.*  
28 **99**, 044109(2002).
- 29 [32] A. Yu. Belov and W.S. Kreher, *Acta Materialia* **54**,  
30 3463(2006).
- 31 [33] J. P. Gong, M. Kawasaki, K. Fujito, R. Tsuchiya, M. Yo-  
32 shimoto, and H. Koinuma, *Phys. Rev. B* **50**, 3280(1994).
- 33  
34  
35  
36  
37  
38  
39  
40  
41  
42  
43  
44  
45  
46  
47  
48  
49  
50  
51  
52  
53  
54  
55  
56  
57